Journal of Power Sources 218 (2012) 88–92

Contents lists available at SciVerse ScienceDirect

Journal of Power Sources

journal homepage: www.elsevier.com/locate/jpowsour

Short communication

High cyclability of ionic liquid-produced TiO_2 nanotube arrays as an anode material for lithium-ion batteries

Huaqing Li [a,b], Surendra K. Martha [a], Raymond R. Unocic [a], Huimin Luo [c], Sheng Dai [d], Jun Qu [a,*]

[a] Materials Science and Technology Division, Oak Ridge National Laboratory, P.O. Box 2008, MS-6063, Oak Ridge, TN 37830-6063, USA
[b] Department of Physics, University of Tennessee, USA
[c] Energy and Transportation Science Division, Oak Ridge National Laboratory, USA
[d] Chemical Sciences Division, Oak Ridge National Laboratory, USA

HIGHLIGHTS

- A proof-of-concept study for using ionic liquid-produced TiO_2 nanotubes (ILNTs) as a novel anode.
- ILNTs contain much less microstructural defects than NTs grown in conventional organic solutions.
- ILNTs demonstrated excellent capacity retention w/o microstructural damage for near 1200 cycles.
- In contrast, conventional TiO_2 NTs pulverized in cycling, resulting in significant capacity fade.

GRAPHICAL ABSTRACT

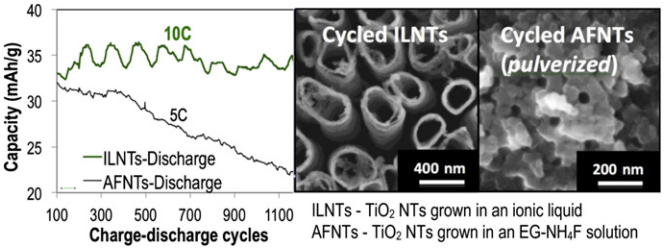

ARTICLE INFO

Article history:
Received 7 June 2012
Received in revised form
26 June 2012
Accepted 28 June 2012
Available online 6 July 2012

Keywords:
TiO_2 nanotubes
Ionic liquids
Lithium-ion battery
Anode
Cyclability

ABSTRACT

TiO_2 nanotubes (NTs) are considered as a potential SEI-free anode material for Li-ion batteries to offer enhanced safety. Organic solutions, dominatingly ethylene glycol (EG)-based, have widely been used for synthesizing TiO_2 NTs via anodization because of their ability to generate long tubes and well-aligned structures. However, it has been revealed that the EG-produced NTs are composited with carbonaceous decomposition products of EG, release of which during the tube crystallization process inevitably causes nano-scale porosity and cracks. These microstructural defects significantly deteriorate the NTs' charge transport efficiency and mechanical strength/toughness. Here we report using ionic liquids (ILs) to anodize titanium to grow low-defect TiO_2 NTs by reducing the electrolyte decomposition rate (less IR drop due to higher electrical conductivity) as well as the chance of the decomposition products mixing into the TiO_2 matrix (organic cations repelled away). Promising electrochemical results have been achieved when using the IL-produced TiO_2 NTs as an anode for Li-ion batteries. The ILNTs demonstrated excellent capacity retention without microstructural damage for nearly 1200 cycles of charge–discharge, while the NTs grown in a conventional EG solution totally pulverized in cycling, resulting in significant capacity fade.

1. Introduction

TiO_2 is of great interest as a promising anode material for Li-ion batteries because it offers enhanced safety, low self-discharge, and good capacity retention on cycling [1–3]. Because of its high operation potential (varying between 1.45 and 1.80 V for different phases) vs. Li^+/Li, the electrode avoids formation of an unstable

* Corresponding author. Tel.: +865 576 9304; fax: +865 574 4913.
E-mail address: qujn@ornl.gov (J. Qu).

0378-7753/$ – see front matter © 2012 Elsevier B.V. All rights reserved.
http://dx.doi.org/10.1016/j.jpowsour.2012.06.096

solid–electrolyte interface (SEI) on the electrode surface and thus eliminates the risk of short circuit caused by dendrites formed in overcharging [4,5]. The SEI-free interface also allows rapid charging and power release. In addition, the small volume change (<4%) of TiO_2 under Li^+ insertion provides high structural stability and potentially good cycling life [1,6]. According to the literature, various nanostructures (nanoparticle, nanowire, nanorod, and nanotube) and different crystalline phases (rutile, anatase, TiO_2-B, TiO_2-R) of TiO_2 are under exploration [7–12]. Among them, anodic self-aligned TiO_2 nanotube arrays (NTs) mitigate the rate-limiting effects of sluggish electron kinetics and mass transport, taking advantage of the large surface area, short diffusion lengths, and orthogonal electron transport paths [13,14].

In the anodizing process, the chemical content of the electrolyte plays a critical role in tube morphology, chemical composition, and crystalline phase [15,16]. The most widely used electrolytes are ethylene glycol (EG)-based, e.g., EG containing NH_4F and H_2O, because of their ability to produce long tubes with uniform diameters and smooth tube walls [17,18]. However, the low-conductivity EG takes a large IR drop during the anodization process and thus decomposes rapidly. The carbonaceous decomposition products are then composited into the TiO_2 matrix during the NTs' growth. The followed crystallization process (annealing) releases the contaminants to inevitably cause nano-scale porosity and cracks, and sometimes tube wall separation [19,20]. These defects are expected to deteriorate the charge transport efficiency and mechanical strength/toughness of the NTs. To overcome these problems, we recently used an ionic liquid (IL), 1-butyl-3-methylimidazolium tetrafluoroborate (BMIM-BF_4), as the electrolyte to fabricate TiO_2 NTs (ILNTs) that have demonstrated less microstructural defects and superior photocatalytic efficiency in water splitting [21]. First, the high-conductivity IL has a small IR drop during anodization resulting in a slow decomposition. Second, the organic cations usually decompose before the inorganic anions, but in anodization the cations are repelled from the NTs that are under a high positive potential. This prevents the ILNTs from compositing with the decomposition products if any.

In this study, we investigated the electrochemical behavior of ILNTs as a candidate anode for the Li-ion battery application and report promising testing results. The ILNTs demonstrated excellent capacity retention and intact structure after nearly 1200 charge–discharge cycles. In contrast, the NTs produced in an EG-NH_4F solution (AFNTs) largely pulverized during cycling, resulting in rapid capacity fade.

2. Experimental

The TiO_2 NTs were produced following the procedure described in our previous work [21]. In brief, titanium foils (125 μm, 99.7%, Sigma) were anodized against a platinum counter electrode using a two-electrode configuration. The IL-based electrolyte contains 98 wt % BMIM-BF_4 (>97.0%, Sigma) and 2 wt. % water. The baseline organic electrolyte is composed of 0.3 wt % NH_4F, 2 wt % H_2O, and the balance EG. All anodizing syntheses were conducted using a DC power supply (E3649A, Agilent) under a constant potential of 50 V for 17 h. All tubes were crystallized using furnace-annealing at 450 °C in air for 3 h with a temperature ramp rate of 1 °C min^{-1} and furnace cooling. Our previous work [21] revealed that both ILNTs and AFNTs are dominated by anatase.

The anode performance of the TiO_2 NTs was evaluated using a two-electrode coin-type half-cell (size CR2032, Hohsen Corp.,

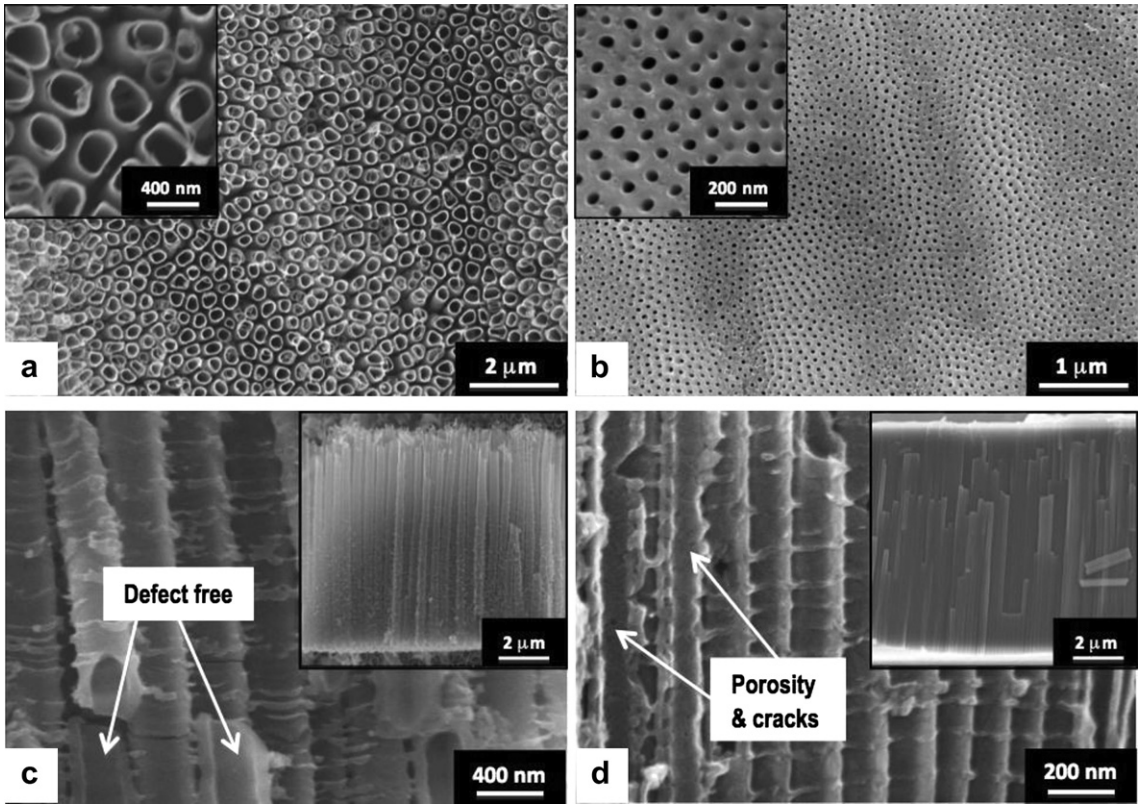

Fig. 1. Top morphology of (a) ILNTs and (b) AFNTs and high-magnification cross-section of (c) ILNTs and (d) AFNTs. Insets in (a) and (b): high-magnification top views. Insets in (c) and (d): low-magnification side views showing tube lengths.

Japan) with a polypropylene membrane separator (type 2325, Celgard, Inc., USA). Lithium foils (purity 99.9%, Alfa Aesar) were used as the counter and reference electrodes. The electrolyte solution was 1.2 M $LiPF_6$ in a 1:2 mixture of ethylene carbonate and dimethyl carbonate by weight (Novolyte Technologies, USA). Cells were assembled in a glove box filled with high-purity argon. After assembly, the cells were stored at room temperature for 12 h to ensure complete impregnation of the electrolyte into the electrodes and separators. Galvanostatic charge–discharge cycling was conducted in a potential range of 1.0–2.5 V using a constant current charge–discharge protocol at rates varying from C/10 (i.e., 10 h for a full charge) to 10 C (i.e., 0.1 h for a full charge) using a multichannel battery tester (Maccor, Inc., model 4000). Cyclic voltammetry (CV) measurements, in a three-electrode half-cell, were carried out using Solartron 1470E and 1455 (Solartron Analytical Ltd., UK) at a scan rate 100 $\mu V\ s^{-1}$ between 3.0 and 1.0 V. Several full sweeps were measured to establish stable performance. In presenting the electrochemical results, current and capacity were normalized by the NTs' mass. The NTs were examined using field emission scanning electron microscopy (Hitachi FE-SEM S4800) and aberration-corrected transmission electron microscopy (FEI Titan S 80-300 TEM/STEM).

3. Results and discussion

Fig. 1 compares the top and cross-sectional morphology of ILNTs and AFNTs. The ILNTs have a much larger tube diameter (OD: 300–400 nm) but a slightly shorter tube length (L: ~8 μm) compared to the AFNTs (OD: 160–200 nm and L: ~9 μm). Similar to our previous report [21], the AFNTs' top surface is covered by a nanoporous debris layer (Fig. 1b), and the tube walls show nanoscale porosity and cracking (Fig. 1d) (due to the release of carbonaceous contaminants in annealing). In contrast, the ILNTs's top surface is free of a debris layer (Fig. 1a), and no microstructural defects are observed in the tube walls (Fig. 1c). The mass per unit area was estimated to be 13.0 and 33.8 mg cm^{-2} for the ILNTs and AFNTs, respectively, based on geometric parameters.

We first investigated the electrochemical behavior by comparing the CV curves of the ILNTs and AFNTs (see Fig. 2). In the first scan, the AFNTs showed two additional small plateaus compared to the ILNTs. The plateaus possibly reflect the residual contaminants and/or microstructural defects in the AFNTs. Both samples after the first scan showed well-defined redox peaks at 1.70–1.74 V and 2.05–2.07 V during cathodic and anodic sweeps, respectively, that are characteristics of Li^+ intercalation ($Ti^{4+} \rightarrow Ti^{3+}$) and deintercalation ($Ti^{3+} \rightarrow Ti^{4+}$) in anatase [22,23].

Fig. 3a and b show the charge–discharge profiles at different rates for ILNTs and AFNTs, respectively. The discharge potential plateau between 1.70 and 1.78 V corresponds to Li-ion insertion, consistent with the previous reports [8,13] of anatase TiO_2 as the starting electroactive material. The charge capacities of the ILNTs were 146, 125, 100, 79, 39, and 35 mAh g^{-1} at the rates of 0.1, 0.2, 0.5, 1, 5, and 10 C, respectively. In comparison, the charge capacities of the AFNTs were 107, 63, 56, 50, 42, and 34 mAh g^{-1} at the rates of 0.1, 0.2, 0.5, 1, 2, and 5 C, respectively.

The galvanostatic cycling performance of the AFNTs and ILNTs at different current rates for the initial 100 cycles is plotted in Fig. 3c. The AFNTs' capacity decreased quickly at the beginning of cycling at C/10 (30% capacity loss from the second to the eleventh cycle) and became relatively stable between 12 and 100 cycles. The dramatic decrease during the first several cycles is possibly due to side reactions with the physical adsorbed water molecules in the TiO_2 nanotubes. Consequently, the side reaction may artificially increase the capacity, but the effect will be eliminated after the consumption of the residual water during the subsequent cycling [24,25]. The ILNTs also showed capacity reduction during the first 4 cycles but soon stabilized after that. This suggests less water adsorbed on the ILNTs probably because of less porosity and cracks (see Fig. 1c).

Fig. 3d shows the cycling behavior after the first 100 cycles until the end of the tests (nearly 1200 cycles). The AFNTs were cycled at 5 C and the ILNTs at 10 C. It can be clearly seen that the cycling performance of the ILNTs at 10 C was better than that of the AFNTs at 5 C, indicating higher-efficiency solid state diffusion of Li-ion in the ILNTs. The capacity of the AFNT electrode consistently declined after 380 cycles, causing an additional 35% capacity loss by the end of cycling. In contrast, the ILNT electrode well retained its capacity with literally no capacity loss between 100 and 1200 cycles, suggesting an excellent long-term cycling life. This has been confirmed by the morphology examination. The morphology of the ILNT and AFNT electrodes after nearly 1200 charge–discharge cycles is shown in Fig. 4. The AFNTs were totally destroyed with most of the tubes pulverized and only few tube roots left on the surface (Fig. 4b). This is because the already defected AFNTs prior to the test (Fig. 1d) could not sustain the fatigue-type lattice strains induced by Li-ion insertion and extraction in cycling. Encouragingly, the ILNTs were intact after the nearly 1200 cycles of charge and discharge (comparing Fig. 4a with Fig. 1a), reflected by their superior capacity retention show in Fig. 3d. Fig. 4c shows a transmission electron microscope image and electron diffraction pattern of the ILNTs after cycling. The three major diffraction rings correspond to anatase 101, 004,

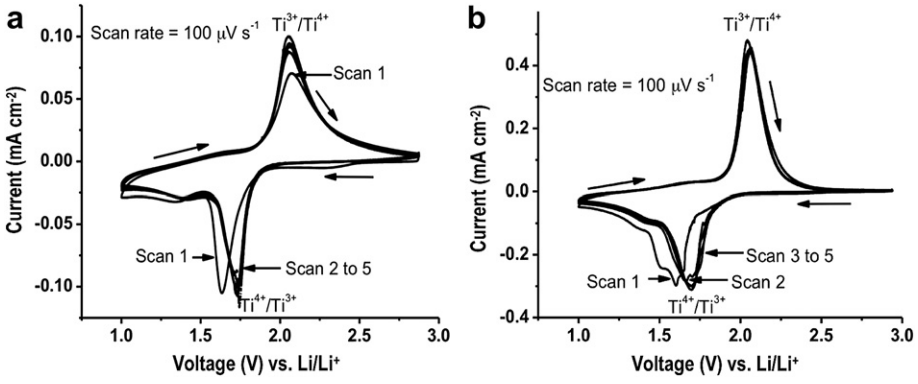

Fig. 2. Cyclic voltammetry curves of (a) ILNTs and (b) AFNTs at a scan rate of 100 $\mu V\ s^{-1}$.

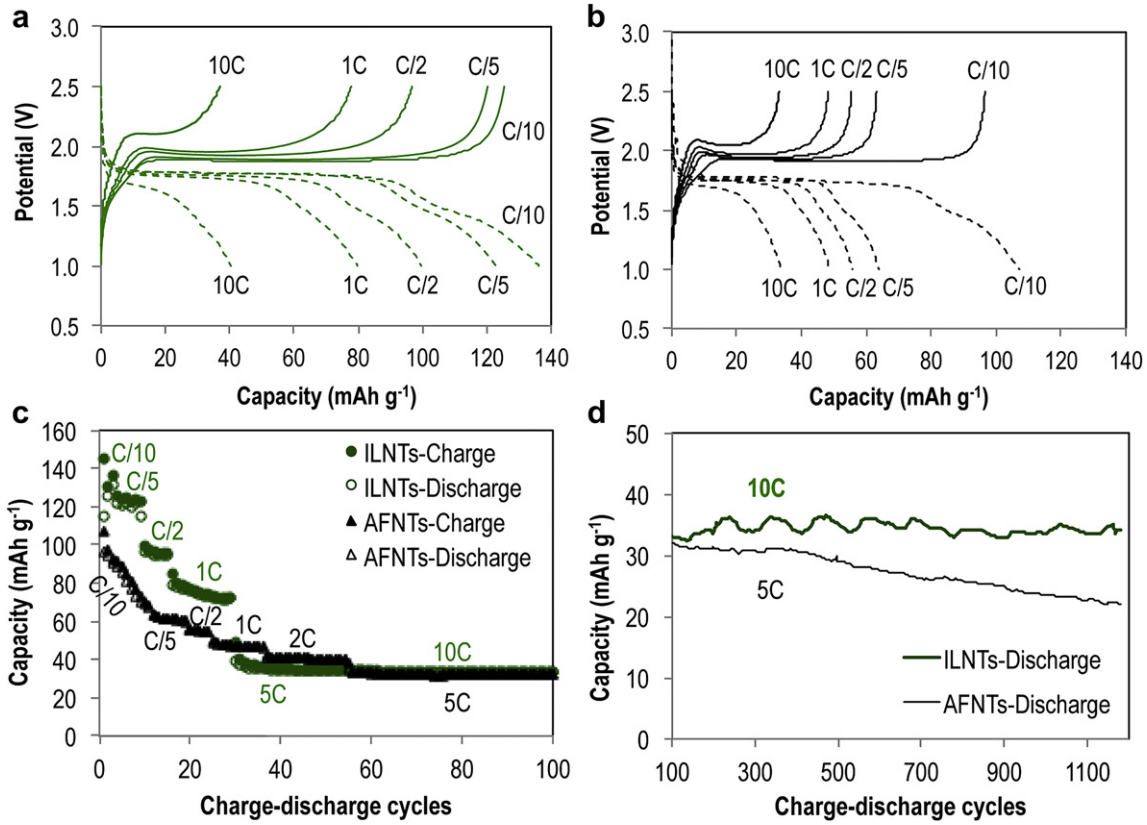

Fig. 3. Charge–discharge profiles at various rates for (a) ILNTs and (c) AFNTs; capacity retention at various charge rates for (c) initial 100 cycles and (d) 100–1200 cycles.

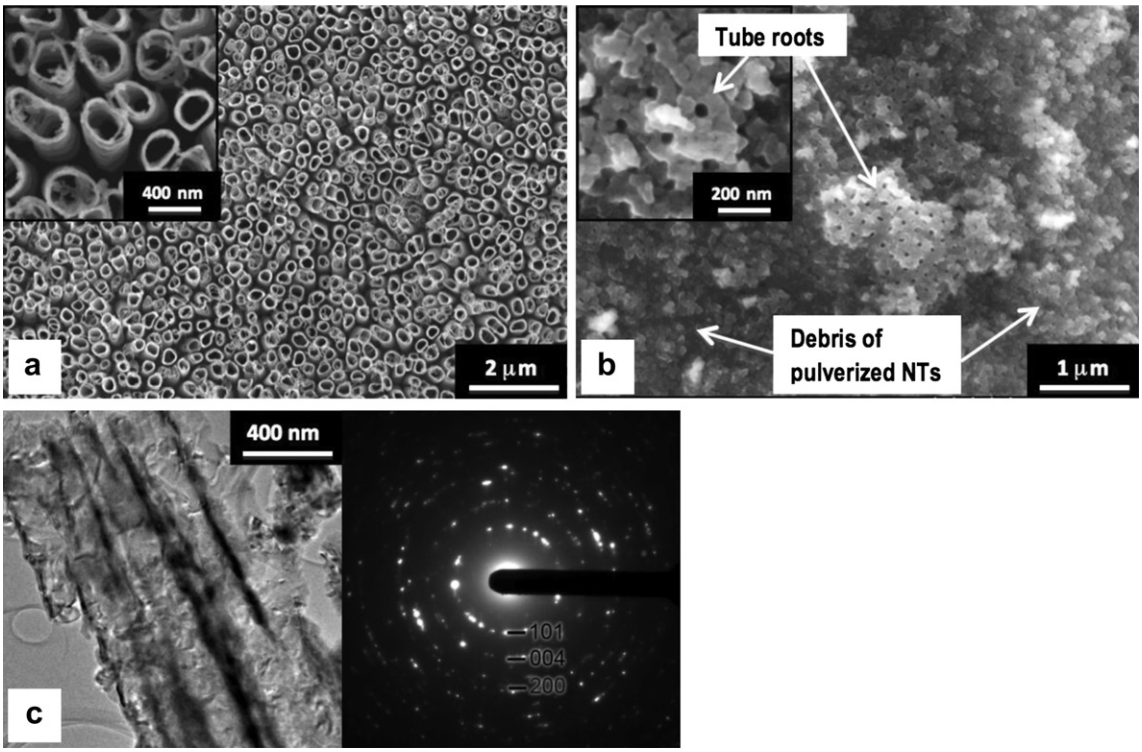

Fig. 4. Morphology of (a) ILNTs and (b) AFNTs after nearly 1200 charge–discharge cycles (insets show high-magnification top views); (c) Transmission electron microscope image (left) and electron diffraction pattern of ILNTs after cycling.

and 200, which indicate no major phase transformation (remaining anatase-dominant) after the large number of cycles of Li-ion insertion and extraction.

4. Conclusion

IL-produced TiO_2 NTs have demonstrated excellent anode characteristics in electrochemical evaluations for the Li-ion battery application. Unlike AFNTs experienced linear capacity fade after 380 cycles and totally pulverized after the cycling test, ILNTs retained the capacity very well for nearly 1200 cycles without noticeable material damage. The superior cyclability of ILNTs is attributed to their low microstructural defects, as a result of using the high-conductivity IL as the anodization electrolyte in the NTs synthesis.

Acknowledgment

The authors thank Drs. Nancy J. Dudney and Jagjit Nanda from Oak Ridge National Laboratory for technical discussion and facility support. Research is sponsored by the US Department of Energy, EERE Industrial Materials Program, under the American Recovery and Reinvestment Act. The characterization work was supported in part by ORNL's SHaRE User Facility, which is sponsored by the DOE Office of Basic Energy Sciences.

References

[1] X. Su, Q. Wu, X. Zhan, J. Wu, S. Wei, Z. Guo, J. Mater. Sci. 47 (2012) 2519–2534.
[2] Z. Yang, J. Zhang, M.C.W. Kintner-Meyer, X. Lu, D. Choi, J.P. Lemmon, J. Liu, Chem. Rev. 111 (2011) 3577–3613.
[3] C. Natarajan, K. Setoguchi, G. Nogami, Electrochim. Acta 43 (1998) 3371–3374.
[4] W.-H. Ryu, D.-H. Nam, Y.-S. Ko, R.-H. Kim, H.-S. Kwon, Electrochim. Acta 61 (2012) 19–24.
[5] D.V. Bavykin, J.M. Friedrich, F.C. Walsh, Adv. Mater. 18 (2006) 2807–2824.
[6] M. Wagemaker, G.J. Kearley, A.A. van Well, H. Mutka, F.M. Mulder, J. Am. Chem. Soc. 125 (2002) 840–848.
[7] H. Xiong, M.D. Slater, M. Balasubramanian, C.S. Johnson, T. Rajh, J. Phys. Chem. Lett. 2 (2011) 2560–2565.
[8] J. Xu, C. Ha, B. Cao, W.F. Zhang, Electrochim. Acta 52 (2007) 8044–8047.
[9] S.-J. Bao, Q.-L. Bao, C.-M. Li, Z.-L. Dong, Electrochem. Commun. 9 (2007) 1233–1238.
[10] Y. Lan, X.P. Gao, H.Y. Zhu, Z.F. Zheng, T.Y. Yan, F. Wu, S.P. Ringer, D.Y. Song, Adv. Funct. Mater. 15 (2005) 1310–1318.
[11] M. Hibino, K. Abe, M. Mochizuki, M. Miyayama, J. Power Sources 126 (2004) 139–143.
[12] A. Kuhn, R. Amandi, F. GarcÂõa-Alvarado, J. Power Sources 92 (2001) 221–227.
[13] G.F. Ortiz, I. Hanzu, T. Djenizian, P. Lavela, J.L. Tirado, P. Knauth, Chem. Mater. 21 (2008) 63–67.
[14] D.-W. Wang, H.-T. Fang, F. Li, Z.-G. Chen, Q.-S. Zhong, G.Q. Lu, H.-M. Cheng, Adv. Funct. Mater. 18 (2008) 3787–3793.
[15] S. Yoriya, C.A. Grimes, J. Mater. Chem. 21 (2011).
[16] A. Ghicov, P. Schmuki, Chem. Commun. (2009).
[17] H.E. Prakasam, K. Shankar, M. Paulose, O.K. Varghese, C.A. Grimes, J. Phys. Chem. C 111 (2007) 7235–7241.
[18] J.M. Macak, H. Tsuchiya, L. Taveira, S. Aldabergerova, P. Schmuki, Angew. Chem. Int. Ed. 44 (2005) 7463–7465.
[19] Y. Ji, K.-C. Lin, H. Zheng, J.-j. Zhu, A.C.S. Samia, Electrochem. Commun. 13 (2011) 1013–1015.
[20] S.P. Albu, A. Ghicov, S. Aldabergenova, P. Drechsel, D. LeClere, G.E. Thompson, J.M. Macak, P. Schmuki, Adv. Mater. 20 (2008) 4135–4139.
[21] H. Li, J. Qu, Q. Cui, H. Xu, H. Luo, M. Chi, R.A. Meisner, W. Wang, S. Dai, J. Mater. Chem. 21 (2011).
[22] J. Wang, Y. Zhou, Y. Hu, R. O'Hayre, Z. Shao, J. Phys. Chem. C 115 (2011) 2529–2536.
[23] D. Fattakhova-Rohlfing, M. Wark, T. Brezesinski, B.M. Smarsly, J. Rathouský, Adv. Funct. Mater. 17 (2007) 123–132.
[24] Z.W. Zhao, Z.P. Guo, D. Wexler, Z.F. Ma, X. Wu, H.K. Liu, Electrochem. Commun. 9 (2007) 697–702.
[25] H. Kim, M.G. Kim, T.J. Shin, H.-J. Shin, J. Cho, Electrochem. Commun. 10 (2008) 1669–1672.